Energy Economics 126 (2023) 107012

Contents lists available at ScienceDirect

Energy Economics

journal homepage: www.elsevier.com/locate/eneeco

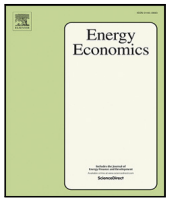

Climate models underestimate the sensitivity of Arctic sea ice to carbon emissions

Francis X. Diebold [a,*,1], Glenn D. Rudebusch [b,1]

[a] University of Pennsylvania, United States of America
[b] Brookings Institution, United States of America

ARTICLE INFO

JEL classification:
Q54
C22

Keywords:
Arctic sea ice area
Climate change
Climate prediction

ABSTRACT

Arctic sea ice has steadily diminished as atmospheric greenhouse gas concentrations have increased. Using observed data from 1979 to 2019, we estimate a close contemporaneous linear relationship between Arctic sea ice area and cumulative carbon dioxide emissions. For comparison, we provide analogous regression estimates using simulated data from global climate models (drawn from the CMIP5 and CMIP6 model comparison exercises). The carbon sensitivity of Arctic sea ice area is considerably stronger in the observed data than in the climate models. Thus, for a given future emissions path, an ice-free Arctic is likely to occur much earlier than the climate models project. Furthermore, little progress has been made in recent global climate modeling (from CMIP5 to CMIP6) to more accurately match the observed carbon-climate response of Arctic sea ice.

1. Introduction

Climate change and rising average surface temperatures are progressing more rapidly in the Arctic than elsewhere. In particular, the loss of Arctic sea ice coverage has been precipitous, especially when measured at the end of the summer melt season. Currently, about half as much of the Arctic ocean is covered by sea ice in September compared to when Arctic ice satellite measurements began 40 years ago (Notz and Stroeve, 2018). The swiftly changing Arctic environment is both a stark indicator of climate change and, in turn, a contributing factor affecting the future evolution of the *global* climate system. The dramatic reshaping of the Arctic – with melting sea ice, ice sheets, and permafrost – will have important influences on the pace and extent of climate change worldwide. For example, with reduced sea ice coverage and more open ocean, less of the sun's radiation is effectively reflected back into space. This reduced sea ice albedo effect promotes increased global temperatures and feeds back to further Arctic melting (Stroeve and Notz, 2018).

An invaluable tool for understanding climate dynamics in recent decades has been the evolving collection of large-scale global climate models. Such models capture the fundamental physical drivers of the earth's climate through a granular, high-frequency accounting of the dynamics of the Earth's atmosphere, oceans, and surface. These structural models have been very useful for a variety of tasks such as uncovering climate variation, determining event and trend climate attribution, and assessing alternative climate scenarios. However, some of the most dramatic Arctic changes evident in the observed data have been poorly captured by large-scale climate models. Notably, these climate models have generally underestimated the amount of lost sea ice in recent decades (Stroeve et al., 2007, 2012; Jahn et al., 2016; Rosenblum and Eisenman, 2017) and Diebold and Rudebusch, 2022. Such discrepancies imply that the climate models do not yet adequately describe the underlying physical processes and feedback mechanisms in the Arctic. This failure could have far-reaching implications for the performance and predictive ability of the global climate models — both in the Arctic and elsewhere.

To better understand the gap between the actual observations and climate model representations of Arctic dynamics, we examine the linear bivariate relationship between sea ice coverage and carbon dioxide (CO_2) levels. This relationship in the observed data has been described by others for both atmospheric CO_2 concentration (e.g., Johannessen, 2008) and cumulative anthropogenic CO_2 emissions (e.g., Notz and Stroeve, 2016). Indeed, the IPCC Sixth Assessment Report (IPPC, 2023) summarizes the research literature on this issue by noting that there is "high confidence" that satellite-observed Arctic sea ice area is strongly correlated with cumulative CO_2 emissions. This strong Arctic sea ice carbon sensitivity – a defining characteristic of the observed data – has been used to assess the Arctic performance of recent vintages of climate models using their simulations conducted for the Coupled

* Corresponding author.
E-mail addresses: fdiebold@sas.upenn.edu (F.X. Diebold), glenn.rudebusch@gmail.com (G.D. Rudebusch).
[1] Contributed equally to all parts of the work.

https://doi.org/10.1016/j.eneco.2023.107012
Received 16 May 2022; Received in revised form 17 July 2023; Accepted 29 August 2023
Available online 6 September 2023

Model Intercomparison Project, phases 5 (CMIP5) and 6 (CMIP6). These two vintages are highly-regarded sources for international global climate model simulations. Notz and Stroeve (2016) show that most CMIP5 models display a lower sensitivity than the observational record. Similarly, Notz (2020) show that most CMIP6 models also fail to simulate the extent of the observed relationship between sea ice and CO_2 emissions.

We extend this research and use a more formal statistical approach that regresses Arctic sea ice on cumulative CO_2 emissions to assess the congruence of observations and models. Specifically, we examine the strength of the Arctic sea ice carbon sensitivity in observed and model-simulated data to better understand the past and future trajectory of Arctic climate change. This analysis provides a useful characterization of the actual observed data and a straightforward benchmark for assessing the ability of the global climate models to account for and predict Arctic sea ice loss.

The substantial differences between estimated statistical representations and the CMIP5 or CMIP6 climate models suggest that the climate models do not adequately capture the underlying physical processes and feedback mechanisms in the Arctic. Of course, the connection between anthropogenic greenhouse gas (GHG) emissions and sea ice coverage is very complex. Atmospheric GHG affect air and ocean temperature and circulation patterns, cloud cover and albedo, and precipitation — all with varying seasonality. As a result, there is still much uncertainty as to why the large-scale climate models fail to capture the extent of the overall downward trend in Arctic sea ice. For example, Guarino et al. (2020) argue that a better representation of the lower surface albedo of summer melt ponds is needed to account for greater incoming shortwave flux. Alternatively, Notz and Stroeve (2016) argue that the climate models underestimate the increase in the incoming longwave radiation for a given increase in CO_2. Similarly, Notz and Stroeve (2016) downplay the role of oceanic heat transport.

Our paper is related not only to earlier work by others, some of which we have already cited, but also to our own earlier work. This paper and Diebold and Rudebusch (2022) have some broad similarity but also very important differences. The broad similarity is that both are concerned (in the context of Arctic sea ice) with evaluating the performance of global climate models, by comparing aspects of model simulations to the corresponding aspects of the observational data. The Diebold and Rudebusch (2022) evaluation compares climate model forecasts to statistical trend forecasts focusing on projected arrival dates of a near ice-free Arctic (NIFA).[2] These NIFA arrival dates differ substantially between the statistical representation (early NIFA) and the climate models (late NIFA), but the question remains as to *why* these projections diverge.

In this paper, we start to address the "why", using a very different approach that does not focus on forecasting. It is more structural, regressing sea ice on a key science-based covariate, cumulative carbon emissions, rather than on a black-box "time trend", in keeping with the broad scientific consensus of a linear ice-emissions relationship. Specifically we compare the carbon-sensitivity of sea ice in climate models and in the observational data. Rather than comparing projected NIFA arrival dates, we document that the climate models show insufficient carbon sensitivity. This result calls for a re-examination of the drivers of ice-emissions relationships in dynamic climate models, which the statistical forecasting analysis of Diebold and Rudebusch (2022) could not reveal.

We proceed as follows. In Section 2, we characterize Arctic sea ice carbon sensitivity in observed data. In Section 3, we characterize Arctic sea ice carbon sensitivity in leading CMIP5 models, and we compare it to that in the observed data. In Section 4, we focus on Arctic sea ice sensitivity in CMIP6 models, assessing not only their agreement with the observed data, but also whether their sea ice sensitivity improves on the earlier-vintage CMIP5 models. In Section 5 we examine whether "bias correction" helps to improve the congruence between data-based and model-based sea ice sensitivity, as is sometimes suggested. We conclude in Section 6.

2. Arctic sea ice carbon sensitivity in the historical record

Various researchers – notably, Johannessen (2008), Notz and Stroeve (2016), and Stroeve and Notz (2018) – have identified a linear empirical relationship between observed Arctic sea ice coverage and atmospheric CO_2 concentration or cumulative emissions. This linear relationship, which fits remarkably well in recent decades, can be expressed as

$$ICE_t = \alpha + \beta \cdot CARBON_t + \epsilon_t, \quad (1)$$

where ICE_t is a measure of sea ice coverage, $CARBON_t$ is a measure of accumulated atmospheric CO_2 (in this paper we will focus on cumulative emissions), and ϵ_t represents deviations from the linear fit.[3,4] The regression intercept, α, calibrates the average level of sea ice coverage. The slope, β, provides a broad measure of the climate response of Arctic sea ice. We will refer to β as the Arctic sea ice sensitivity or carbon sensitivity. A negative value of β captures the diminishing coverage of Arctic sea in response to the greater accumulation of greenhouse gases in the atmosphere. Eq. (1) is at the center of our analysis of both the observed historical data and climate model simulations.[5]

For the observed data, we consider several of empirical implementations of Eq. (1) to assess the robustness of the relationship. Some of these variations are shown in Fig. 1, and all data are described in Appendix A. Arctic sea ice area, SIA, is used as a measure of ICE_t. Arctic sea ice coverage has been well measured since the end of 1978 using satellite-based passive microwave sensing. For any polar region divided into a grid of individual cells, the satellite readings provide the fraction of ice surface coverage for each cell. SIA is the sum of the ice-covered areas with at least 15% ice coverage — that is, the sum of the fractional cell areas above that minimum.[6] Similar results are obtained using Arctic sea extent, SIE, as a measure of ICE_t, as shown in Appendix B.

In Fig. 1 we show SIA against global cumulative emissions as in Notz and Stroeve (2016) and Stroeve and Notz (2018). We consider three different seasonal measurements of Arctic sea ice coverage, namely, March (in blue) and September (red) and the annual average (black). Taken as a whole, the three alternative regressions in Fig. 1

[2] Also related is Diebold et al. (2023), which continues with forecasting analyses as in Diebold and Rudebusch (2022), but which is not concerned with evaluation of dynamical climate models. Instead it develops and explores extensions, variations, and robustness checks for statistical forecasting models.

[3] Our carbon-trend regression is a cointegrating regression if appropriate, but we do not need to take an explicit stand on non-stationarity. In particular, an OLS carbon-trend regression in levels is consistent regardless of whether the trends are deterministic, stochastic (integrated) but not cointegrated, or integrated and cointegrated (Stock et al., 1990). This result allows us to skirt the unit root minefield, which is helpful because our 40 annual sea ice and carbon observations are not very informative in distinguishing unit roots from nearby alternatives.

[4] Other researchers have examined a similar empirical linear relationship between Arctic sea ice and a measure of global temperature, as in Winton (2011) and Rosenblum and Eisenman (2017).

[5] Matthews et al. (2009) consider a similar proportional relationship between global temperatures and cumulative carbon emissions and the associated temperature climate sensitivity.

[6] In particular, monthly average sea ice data from the National Snow and Ice Data Center (NSIDC) are used, January 1979–December 2019. These data use the NASA team algorithm to convert microwave brightness readings into ice coverage data. Diebold et al. (2021) provide details on data construction and evidence supporting use of NSIDC data.

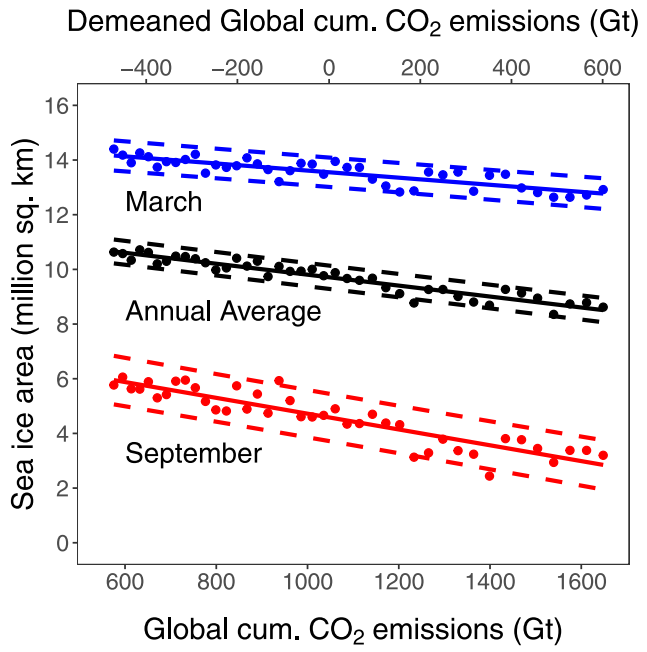

Fig. 1. Arctic sea ice area and CO_2.
Notes: Arctic sea ice area (in million km^2) is shown against global cumulative CO_2 emissions (in Gt). March, annual average, and September observations are shown in blue, black, and red, respectively. Dashed lines are 95% prediction intervals accounting for parameter estimation uncertainty. Carbon scales are shown in both demeaned (top scale) and non-demeaned (bottom scale) forms. The sample period is 1979–2019. See text for details. (For interpretation of the references to color in this figure legend, the reader is referred to the web version of this article.)

display a remarkably consistent linear empirical regularity. In theory, the observed connection between Arctic sea ice and anthropogenic carbon is determined by many different dynamic geophysical channels and feedbacks, including variation in air and water temperature as well as changing surface albedo, cloud cover, wave action, and thermohaline ocean currents. Separately or in combination, these could induce a nonlinear relationship – or even a tipping point – between Arctic sea ice and carbon. Instead, for the past few decades, this relationship can be well approximated as linear.[7] Of course, when sea ice reaches its zero lower bound, this linear relationship will break down as CO_2 levels increase while sea ice – at least, in late summer and early autumn – holds steady at its lower bound of zero coverage.[8] Despite the high likelihood of such future nonlinearities, a linear relationship provides a useful benchmark to capture at a very broad level the current Arctic sea ice carbon sensitivity.

Table 1 reports details for the regressions shown in Fig. 1. The Table 1 results are based on demeaned $CARBON$. The location shift associated with moving from $CARBON$ to demeaned $CARBON$ is of course harmless — just a change of units. Indeed, both $CARBON$ scales are shown simultaneously in Fig. 1, with the demeaned scale along the top of each panel and the original version at the bottom. However, using demeaned $CARBON$ aids with the interpretation and comparison of the regression. In particular, the regression intercept when using demeaned $CARBON$ is the predicted value of SIA at the historical mean of $CARBON$, which is familiar and easily understood. This contrasts with the regression intercept when using non-demeaned $CARBON$, which is the predicted value of SIA at *zero* $CARBON$, far beyond the range of historical experience. Accordingly, demeaned $CARBON$ data are used from this point onward.

The three columns of Table 1 are for September, annual, and March SIA. The table reports three types of information. First, it reports estimates of the intercept and slope coefficients, denoted $\hat{\alpha}$ and $\hat{\beta}$, the coefficient standard errors, and the regression R^2. The slope coefficients, β, summarize Arctic sea ice sensitivity. There is a clear seasonal pattern, with the September slope steeper than the annual average, which in turn is steeper than March. Our estimated September sea ice sensitivity for cumulative carbon emissions is essentially identical to the value in Notz and Stroeve (2016), which was based on a sample from 1953 to 2015.[9] The strong linear relationship between the sea ice coverage and carbon forcing – evident visually in Fig. 1 – is reflected numerically in the small standard errors and high R^2's (more than 80%) of Table 1.

Second, Table 1 reports three simple diagnostic test statistics for various aspects of adequacy of the basic regression model (1). The first, labeled "H_0: Linear regression relationship" is a t-test of the fitted linear relationship against a nonlinear (quadratic) alternative; that is, a t-test of the coefficient on $CARBON^2$ when added to regression (1). The second, labeled "H_0: Stable regression relationship", is a Quandt (1960) F-test of a stable linear relationship against the alternative of a broken linear relationship, with a mid-sample break in 2000. The third, labeled "H_0: Gaussian regression disturbances", is a Kiefer and Salmon (1983) χ^2 test of Gaussian disturbances against an arbitrary non-Gaussian alternative — effectively a test of skewness = 0 and kurtosis = 3. In every case – across all regression variations and hypothesis tests – there is no evidence that a linear regression is an insufficient representation of the connection between Arctic sea ice and CO_2.

As a final statistic of interest, Table 1 also reports the levels of forcing variables at which the linear regressions predict the effective disappearance of September Arctic sea ice — a nearly ice-free Arctic (NIFA), which is defined as only 1 million km^2 of sea ice remaining.[10] The NIFA levels are based on extrapolations of the linear regressions until the effectively ice-free coverage benchmark is reached. A September NIFA is reached with cumulative CO_2 emissions of 2287 Gt, which is almost 650 Gt greater than the 2019 observed level of 1648 Gt.[11] Table 1 also shows that this NIFA level of CO_2 emissions will be reached in 2032 or 2034 based on the "Shared Socioeconomic Pathways" SSP3-7.0 or SSP2-4.5. These are two plausible climate scenarios that are widely used as inputs in climate model simulations, especially for assessment reports by the Intergovernmental Panel on Climate Change (IPCC). Taken together, the results in Table 1 – assuming a standard extrapolation of future emissions – predict an essentially ice-free September Arctic Ocean will likely occur about a decade from now. This timing is broadly consistent with the statistical projections in Diebold and Rudebusch (2022), Diebold et al. (2023), and other analyses.[12]

[7] Notz and Stroeve (2016) argue that such linearity can be motivated from a simple conceptual model of the surface energy balance at the sea ice edge.

[8] Diebold and Rudebusch (2022) discuss the lower bound on sea ice and provide an empirical shadow ice modeling strategy to account for it.

[9] Notz and Stroeve (2016) also provide an intuitive interpretation of the magnitude of estimated September sea ice sensitivity, noting that it translates into a loss of approximately 3.0 m^2 of September Arctic sea ice per metric ton of CO_2 emissions, which allows individuals to easily calculate their own contribution to diminishing sea ice from personal actions.

[10] The definition of NIFA follows the usual convention in the literature as the appropriate definition of an effectively ice-free Arctic, reflecting the hypothesized persistence of residual sea ice clinging to northern coastlines despite an open Arctic ocean (Diebold et al., 2023).

[11] Notz and Stroeve (2018) provide a similar benchmark for reaching NIFA.

[12] Diebold and Rudebusch (2022) found a slightly increasing rate of decline in Arctic sea ice over the past few decades, which is consistent with a linear relationship between sea ice and CO_2, given the past increasing rate of change in emissions, as discussed in Diebold et al. (2023).

Table 1
Regressions of sea ice area on Cumulative CO_2 Emissions.

	Sea ice area		
	September	Annual Average	March
Intercept (million km^2)	4.586	9.713	13.553
	(.066)	(.033)	(.041)
Sensitivity (m^2/t CO_2)	−2.891	−2.000	−1.299
	(.209)	(.103)	(.130)
R^2	.83	.90	.71
H_0: Linear regression relationship	p = .53	p = .95	p = .69
H_0: Stable regression relationship	p = .45	p = .28	p = .84
H_0: Gaussian regression disturbances	p = .52	p = .10	p = .43
NIFA CO_2 level	2287	5403	10713
NIFA Year (SSP2-4.5)	2034		
NIFA Year (SSP3-7.0)	2032	2080	

Notes: Shown are regression estimates of Arctic sea ice area on demeaned cumulative CO_2 emissions since 1850 with coefficient standard errors are in parentheses. Sensitivity or slope coefficients are shown in m^2 per ton of CO_2 (which is equivalent to thousands km^2 per Gt CO_2). Also shown are p-values for tests of three hypotheses: a linear relationship against a quadratic alternative, a linear relationship against a broken linear alternative with mid-sample break point, and Gaussian disturbances against an arbitrary non-Gaussian alternative. Extrapolated dates of a nearly ice-free Arctic (NIFA) and the associated CO_2 levels assuming SSP2-4.5 and SSP3-7.0 scenario paths are also shown. The sample period is 1979–2019.

3. CMIP5 models have low arctic sea ice sensitivity

In this section, the observed Arctic sea ice data are compared to individual CMIP5 climate model simulation paths through the lens of the linear sea ice sensitivity regression of ICE on $CARBON$ given in Eq. (1). That is, sea ice sensitivity regressions are fit to observed historical data and dynamic model paths. In particular, we focus on the September sensitivity regression of SIA on cumulative CO_2 emissions, as in Notz and Stroeve (2016), and give attention is both the sensitivity (regression slope) and predicted ICE at mean $CARBON$ (regression intercept).

The observational data are summarized by the linear regression estimates given in Table 1, as discussed earlier. The intercept and slope estimates are shown as a red square in Panel A of Fig. 2, together with a 95% confidence ellipse under normality.[13] These two values (e.g., for September data, $\hat{\alpha} = 4.586\ 10^6$ km and $\hat{\beta} = -2.891$ m^2/t) will be the key summary statistics for Arctic sea ice climate dynamics that we will use to assess the global climate models.

We first examine the conformity of these estimates with analogous values from 37 different CMIP5 models. All of these climate models were simulated with a common path of cumulative global CO_2 emissions and produced simulated data on Arctic sea ice. For a single simulation of each model, we use the generated 1979–2019 data sample of emissions and Arctic sea ice area to estimate the Arctic sea ice sensitivity regression.[14] The resulting 37 linear regression intercept and slope estimates – one pair for each CMIP5 model – are shown as black circles with black confidence ellipses obtained from the sampling uncertainty associate with each simulation.

All of the resulting estimates are shown in Fig. 2, which provides a straightforward assessment of whether the black model-based coefficients match the red data-based coefficients. Panel A of the figure focuses on the September Arctic sea ice sensitivity regressions. Comparing model regression results to results with observed data, only two of the 37 black model parameter point estimates – those for the CNRM-CM5 and HadGEM2-CC models – are inside the red data ellipse. Indeed, for the vast majority of models, the entire black model ellipse has no intersection with the red data ellipse. Non-overlapping model-based and data-based ellipses indicate that with high probability the population model-based coefficients do not match those governing the observed data, even after accounting for the uncertainty in both estimates.

If clear disagreement between models and data is revealed by Panel A of Fig. 2, so too is the nature of the disagreement. There are three key aspects. First, the estimated model intercepts have a "bias problem", with most of the model estimates too high. As evidenced by the distributional notches on the horizontal axis, 30 of the 37 black model estimates are to the right of the vertical red line. That is, the models tend to be mis-calibrated in terms of the level of sea ice: *September Arctic sea ice at historical mean carbon is too high in the models*.

Second, the estimated model slopes also have a bias problem. In absolute value, the slope estimates are biased downward with 32 out of 37 black model dots above the horizontal red line. The data-based slope estimate is approximately −3 m^2 – an additional tonne of cumulative emissions causes sea ice loss of 3 m^2 – whereas the model-based slope estimates are centered near −2 m^2. That is, the models tend to be mis-calibrated not only in terms of too much sea ice on average but also in terms of the weak absolute response of sea ice to increases in cumulative carbon emissions: *the response of September Arctic sea ice to increases in carbon is too small in the models*.

Finally, the figure also makes clear that in addition to being centered in the wrong place, the model-based estimates also have a variance problem. This is particularly apparent for the distribution of intercepts shown by the notches on the horizontal axis: *September Arctic sea ice at historical mean carbon varies disturbingly widely across models*. The intercepts vary from below 2 million km^2 to above 9 million km^2. The model-based slope estimates have a relatively lower-variance, while the intercept estimates are both high-bias *and* high-variance.

Panel B of Fig. 2 presents a similar comparison but using annual average data, rather than just September. In principle, the models could perform better at matching Arctic ice dynamics over the whole year and still miss the September lows. Instead, the intercept bias and intercept variance problems remain, as does the slope bias problem. Hence the divergence between models and data is not just a September or a seasonal issue, but the biases in the climate models appear more pervasive.

Only one run from each CMIP5 model was shown in Fig. 2, as in Notz and Stroeve (2016). However, 12 of the 37 models have multiple runs available, i.e., *ensembles* of simulations. We have replicated our regression analysis on all of the simulations from these models, and

[13] The confidence ellipses are not tilted with a demeaned carbon series. Since the independent variable is transformed to have zero mean, the sampling uncertainty in the estimation of the slope does not alter estimation of the intercept, and the lack of covariance between the slope and intercept estimate leads to non-tilted ellipses.

[14] The data for the CMIP5 model simulations are detailed in Notz and Stroeve (2016) and Appendix A. In particular, Fig. 2 employs the only model run or the first run of any model ensemble under RCP8.5. Detailed CMIP5 regression results are provided in Appendix C.

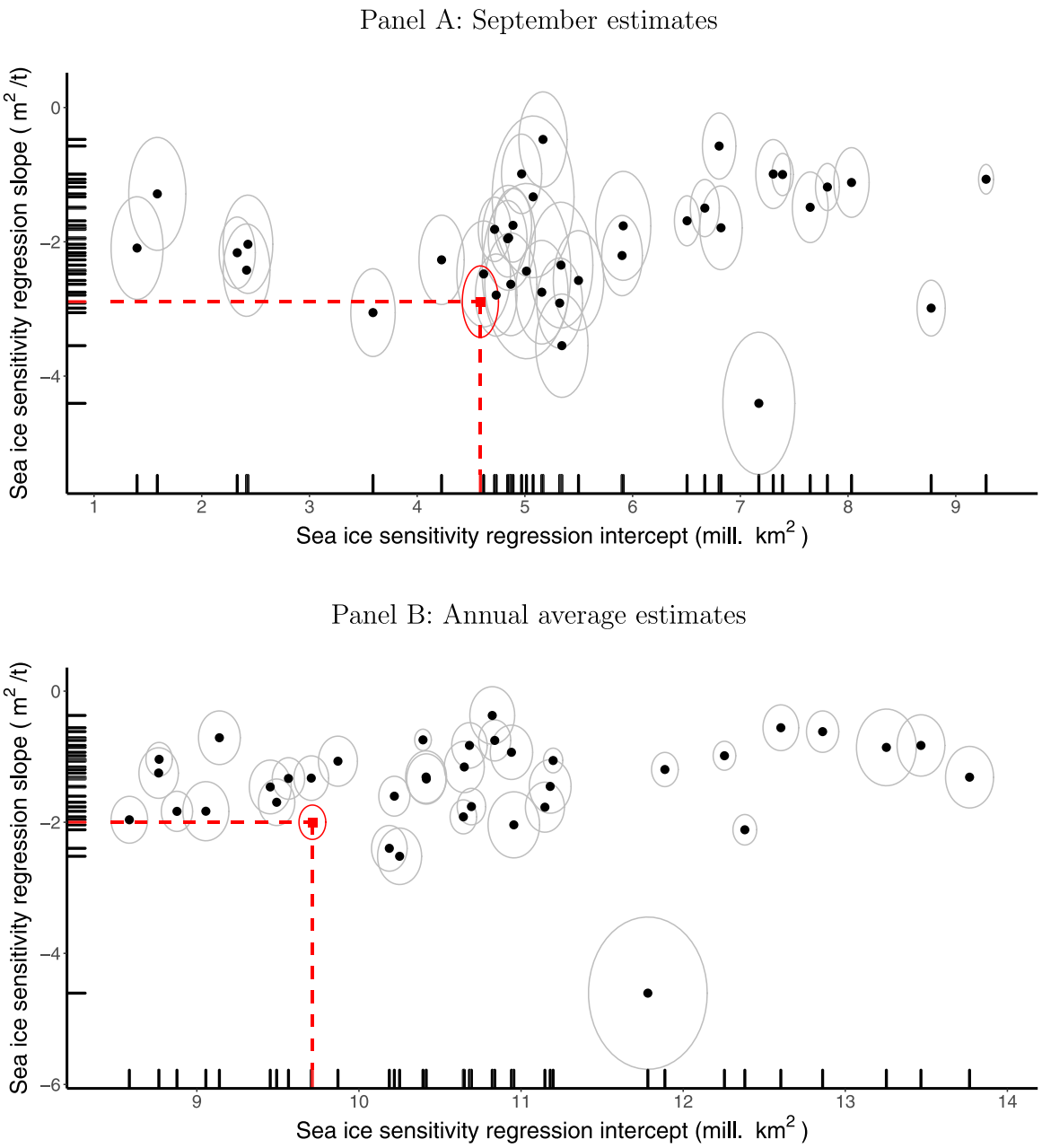

Fig. 2. Model and observed sea ice sensitivity, estimates from single runs of 37 CMIP5 models.
Notes: Sea ice sensitivity regression intercepts and slopes estimated from the observed data (1979–2019) are shown as a red square, with a 95% confidence ellipse. Sea ice sensitivity regression intercepts and slopes are shown as black circles, again with 95% confidence ellipses. The notches on the axes provide information about marginal distributions. See text for details.

in Fig. 3, intercept and slope estimates from these ensembles of model runs are shown for the 12 models. The estimated intercept–slope pairs from the multiple runs of a single model are all give a unique symbol, and the number of runs in each model's ensemble is reported in the figure key. Taken as a whole, these 50 runs tell the same story as before. Taken as a whole, the multi-run ensembles do just as poor of a job of matching the observational data as regards the connection between Arctic sea ice and carbon emissions. In particular, (1) Arctic sea ice at historical mean carbon is too high in most models, (2) the response of Arctic sea ice to increases in carbon is too weak in most models, and (3) Arctic sea ice at historical mean carbon varies wildly across models.

The multiple runs in Fig. 3 also allow us to address the issue of internal variability. Internal variability refers to variations over time in measures of climate resulting from natural causes. In climate models, internal variability is caused by the climate system's chaotic nature coupled with slight perturbations in initial conditions. If, for example, the estimated coefficient pairs for all of the models were distributed evenly throughout Fig. 3, that might suggest that the confidence ellipses based on single simulations generally underestimated the actual climate variation generated by the models.[15] Instead, all of the coefficient estimates for a given model are clustered together, indicating that our regression estimates are generally robust to internal variability. As in Notz and Stroeve (2016), the Arctic sea ice carbon sensitivity we estimate is based on the average climatic conditions over several decades, which moderates the influence of internal variability to a substantial degree. Indeed, the multiple simulations in Fig. 3 tell much

[15] Olonscheck and Notz (2017) argues that internal variability can account for much of the poor fit of climate models to Arctic sea ice.

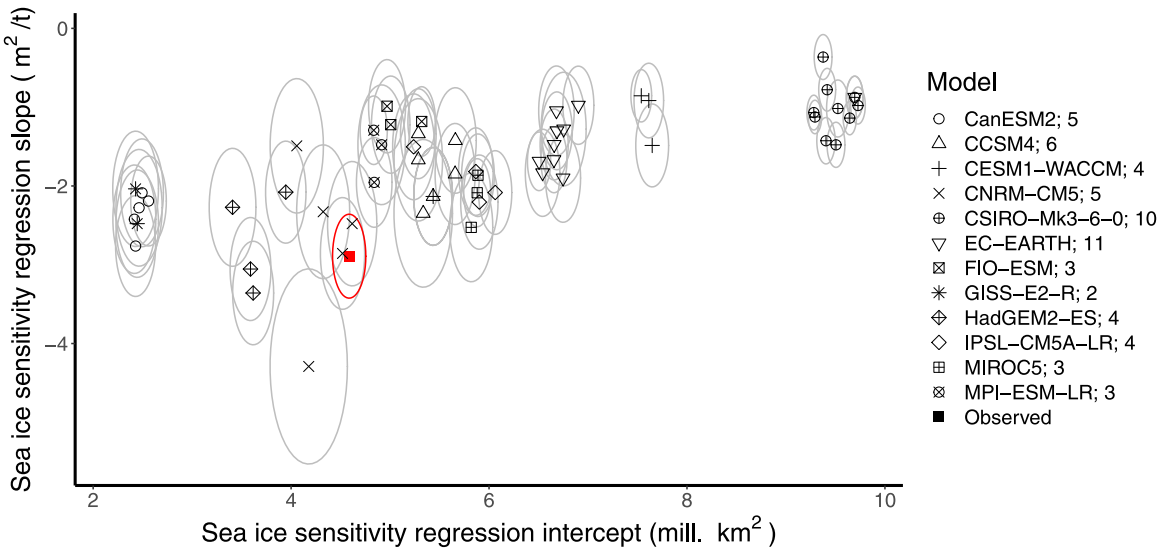

Fig. 3. Model and observed sea ice sensitivity, ensemble estimates from 12 CMIP5 models.
Notes: Sea ice sensitivity regression intercepts and slopes estimated from the observed data (1979–2019) are shown as a red square, with a 95% confidence ellipse. Sea ice sensitivity regression intercepts and slopes are shown as black circles, again with 95% confidence ellipses. Run 5 of EC-EARTH is not shown because it is an extreme outlier with a positive slope of 2.719 and intercept of 4.802. See text for details.

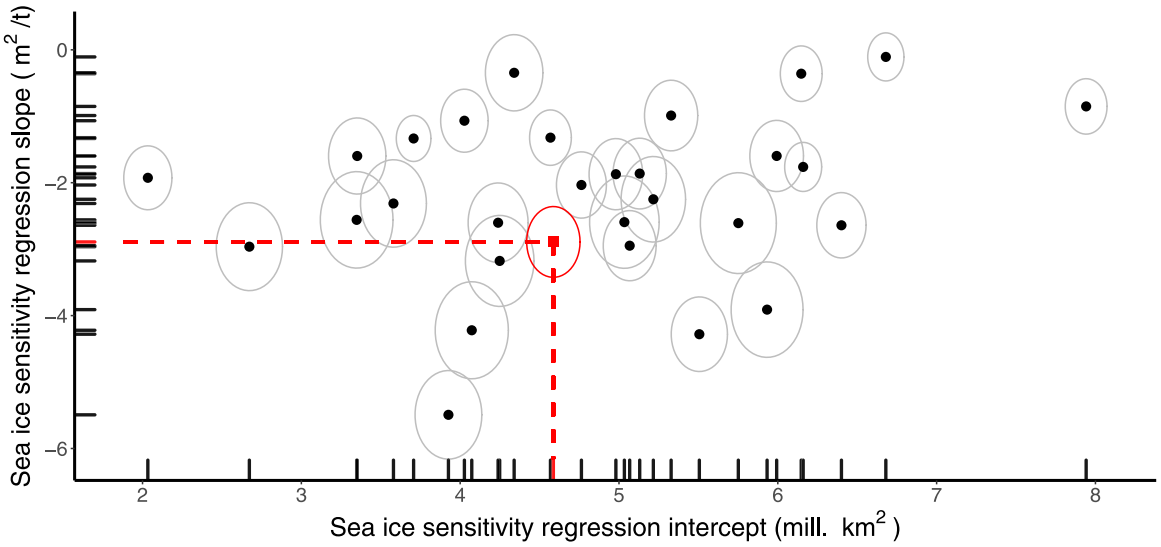

Fig. 4. Model and observed September sea ice sensitivity, single simulation runs of 29 CMIP6 models.
Notes: The sea ice sensitivity regression intercept and slope estimated from the observed September data (1979–2019) are shown as a red square. Sea ice sensitivity regression intercepts and slopes estimated from single simulation runs of 29 different CMIP6 models are shown as black circles. The ellipses are 95% confidence regions for intercept/slope pairs based on sample variability.

the same story as the single runs. Only the same two models – the CNRM-CM5 and HadGEM2-CC models – come close to spanning on average the real-world estimated Arctic sea ice sensitivity slope, though both consistently underpredict the intercept and hence the average level of the sea ice.

4. CMIP6 models do not improve on CMIP5

Simulations from the latest generation of climate models – CMIP6 – have recently become available. Notz (2020) provides an initial overview of these simulations. They conclude that on average the models provide a "more realistic" estimate of the sensitivity of September Arctic sea ice area to cumulative carbon emissions than earlier CMIP models. Here we re-assess that conclusion using the methodology employed above.

Recall the key sensitivity visualization of Fig. 2 (Panel A) for the CMIP5 models, which made clear that Arctic sea ice sensitivity diverges sharply in the data vs. the CMIP5 models. The same visualization is shown in Fig. 4, but for CMIP6 rather than CMIP5 models. The similarity between Figs. 2 and 4 is striking — the CMIP6 models show little improvement on balance over the CMIP5 models in terms of Arctic sea ice sensitivity. No model-based coefficient pair falls in the red ellipse. Intercept bias appears to have been reduced, but at the cost of much more notable dispersion across these estimates. Slope bias seems little reduced, and again, the variance of the estimates has grown.

The CMIP6 ensemble results are equally striking, especially when contrasted directly with the CMIP5 ensemble results. As described in the data appendix, we were able to pair CMIP5 and CMIP6 versions of the same basic model in 6 instances in which we also had a reasonable number of simulations for each phase. These basic models are CanESM, CNRM-CM, EC-EARTH, IPSL-CM, MIROC, and MPI-ESM as shown in

Table 2
Comparison of sea ice sensitivity in CMIP5/6 models and observed data.

Model (CMIP vintage)	$\bar{\alpha} - \alpha^{obs}$	$\bar{\beta} - \beta^{obs}$	$\sigma(\hat{\alpha})$	$\sigma(\hat{\beta})$	#Sims
CanESM2 (CMIP5)	−2.123	0.614	0.057	0.262	5
CanESM5 (CMIP6)	1.277	−0.954	0.268	0.639	49
CNRM-CM5 (CMIP5)	−0.263	0.412	0.232	1.025	5
CNRM-CM6-1 (CMIP6)	0.348	1.773	0.257	0.551	6
EC-EARTH (CMIP5)	2.099	1.591	0.932	1.293	11
EC-Earth3 (CMIP6)	−1.290	0.971	0.420	0.637	31
IPSL-CM5A-LR (CMIP5)	1.298	0.941	0.363	0.311	4
IPSL-CM6A-LR (CMIP6)	−0.881	−0.903	0.325	0.781	6
MIROC5 (CMIP5)	1.293	0.805	0.037	0.337	3
MIROC6 (CMIP6)	0.110	0.993	0.150	0.428	50
MPI-ESM-LR (CMIP5)	0.253	1.414	0.045	0.341	3
MPI-ESM1-2-LR (CMIP6)	−0.572	1.040	0.106	0.365	10
Median of CMIP5 models	0.773	0.873	0.145	0.339	
Median of CMIP6 models	−0.231	0.982	0.262	0.594	

Notes: Top panel: For model simulations, differences of the median model simulation intercept and slope from the observed data estimates are shown, respectively, $\bar{\alpha} - \alpha^{obs}$ and $\bar{\beta} - \beta^{obs}$, 1979–2019. In addition, standard deviations of the model simulation intercept and slope estimates are shown, respectively, $\sigma(\hat{\alpha})$ and $\sigma(\hat{\beta})$. Bottom panel: median values of CMIP5 and CMIP6 median-model results.

Fig. 5. In each panel, the exact versions of the models used are reported in the panel titles. The estimated September Arctic sea ice area response coefficient pairs are given in each panel for the CMIP5 and CMIP6 ensemble simulations. The coefficient pairs from the ensembles of CMIP5 simulations are shown as open circles. and the corresponding pairs from the CMIP6 simulations are shown as solid circles. Of course, given the improvements in modeling and computational speed, there are typically more CMIP6 simulations than CMIP5 simulations in the ensembles. These are detailed in the rightmost two columns of Table 2, so for example, CanESM has 5 runs from CMIP5 and 49 from CMIP6.

On the one hand, as in Panels A, C, D, and E of Fig. 5, the CMIP6 estimates appear to be clustered somewhat closer to observed real-world slope and intercept pair. On the other hand, however, as for the CMIP5 simulations, there is little or no overlap between the CMIP6 simulations and the observed sensitivity ellipses. There are also notable differences in the CMIP5 and CMIP6 sensitivity ellipses. Indeed, the *CMIP5 and CMIP6 simulations appear as distinct clusters, overlapping little or not at all with each other or the observed sensitivity ellipse*. Overcompensation is often apparent, as in Panel A for the CanESM ensembles, whose intercepts desirably increase from CMIP5 to CMIP6, but by too much.

Table 2 provides some summary statistics for the panels of Fig. 5. The first two columns of the table show the distances from the observed intercept and slope estimates (α^{obs} and β^{obs}) to the median estimates from the CMIP5 and CMIP6 simulations ensemble-by-ensemble ($\bar{\alpha}$ and $\bar{\beta}$). The second two columns show the standard errors of the estimated model-based intercept and slope coefficients across simulation runs in each ensemble ($\sigma(\hat{\alpha})$ and $\sigma(\hat{\beta})$). The final two rows give the median of the six CMIP5 statistics and the median of the six CMIP6 statistics for each column.

The intercept bias in the first column, labeled $\bar{\alpha} - \alpha^{obs}$, where positive values correspond to overestimates of the real-world intercept, which results from simulations with too much sea ice on average. As shown in the bottom two rows, the CMIP6 models have reduced this bias; however, as shown by the increased intercept standard errors, variability has also jumped. The sea ice sensitivity differences appear in the second column, labeled $\bar{\beta} - \beta^{obs}$, where positive values correspond to insufficient sensitivity. All CMIP5 models display insufficient sensitivity; the cross-model median $\bar{\beta} - \beta^{obs}$ is 0.87. The CMIP6 models fare no better; four of the six remain insufficiently sensitive, and the other two over-compensate and become overly sensitive. The cross-model CMIP6 median is *worse* than the CMIP5 median, with $\bar{\beta} - \beta^{obs} = 0.98$. The variance of slope estimates evident in $\sigma(\hat{\beta})$ has also risen.

5. Bias correction is not a solution

Our results have illustrated dramatic shortcomings in climate model representations of Arctic sea ice coverage. As noted above, previous research has described related deficiencies in climate model fit and performance. In response, a literature has developed that "bias corrects" climate model simulations. Indeed, bias correction methods of varying sophistication have been used in hundreds of climate change impact studies over the past decade (e.g., Otto et al. (2012), Turner et al. (2013), Melia et al. (2015), Ivanov et al. (2018), and Kusumastuti et al. (2022)). In this section, we argue that such bias corrections are at best a partial fix for climate model projections and that they should not obscure the need for further improvement and progress in climate models.

The bias correction of climate model outputs has been performed using a variety of methods ranging from simple to arcane. The basic goal of a bias correction is to adjust the climate model projection of a particular variable ex post in order to have that projection better match the historical data during some "calibration sample" – and hopefully beyond that as well. For example, a simple "additive" bias correction of a series merely adjusts a model simulation by subtracting the difference between the average of that model's ensemble of simulated data for that series and the average of the observed data over the given calibration sample. That is, each individual model simulation is corrected for the average error across all the simulations in the ensemble. To try to account for the effects of the zero lower bound for sea ice indicators, Melia et al. (2015) also introduce multiplicative bias correction methods based on the ratio of the mean of the model ensemble simulations and the mean of the observed data along with variance corrections.

For the CMIP6 climate model simulations of Arctic sea ice area, we have explored the effects of simple additive bias corrections and the effects of applying the more complicated mean and variance bias correction (MAVRIC) of Melia et al. (2015). For the latter, Fig. 6 provides a representative example using the MPI-ESM1-LR model CMIP6 simulations. Each SIA simulation is adjusted based on the observed bias across the 10 simulations in this model's ensemble from 1979 to 2019. We then use the bias-corrected model simulation SIA paths as data in the sea ice sensitivity regression of Eq. (1). Fig. 6 compares the resulting regression intercept and slope estimates from the original (no bias correction) simulations and the bias-corrected simulations (together with 95% confidence ellipses). Not surprisingly, the application of the bias correction re-centers the intercept estimates so that they

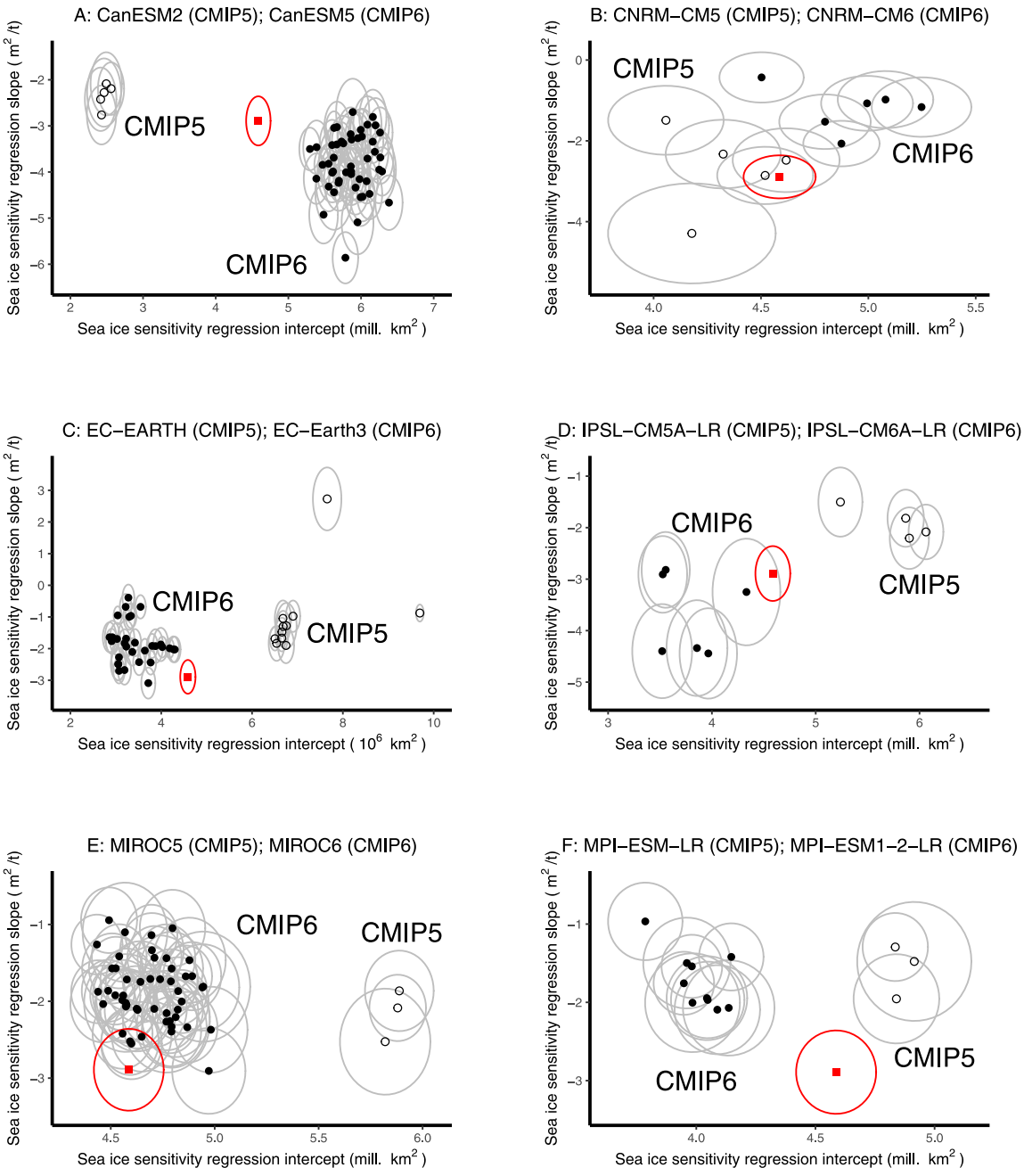

Fig. 5. September sea ice sensitivity results for CMIP5/6 paired models.
Notes: The sea ice sensitivity regression intercept and slope for the observed September data (1979–2019) are denoted by a red square. Similar intercepts and slopes estimated from single simulation runs of two different models are shown as black circles — CMIP5 as open circles and CMIP6 as solid circles. Each ellipse is a 95% confidence interval for a coefficient pair based on sample variability.

line up with the historical intercept on average. That is, the bias-corrected simulation intercept estimates do more closely match the observed intercept of the historical series — the white dots are better centered vertically with red square. However, the bias correction has not tempered the wide variance of intercept estimates for individual simulations. More seriously, the slope estimates remain wildly off the mark from a historical perspective, so the bias correction has done nothing to eliminate the problem of the relative insensitivity of Arctic sea ice conditions to CO_2. We obtained similar results with other models and bias correction methods.

Fig. 6 illustrates a longstanding trenchant criticism of the use of bias correction in the climate modeling literature (e.g., Ehret et al. (2012) and François et al. (2020)). Namely, because bias correction almost invariably focuses on a single variable, it cannot correct a climate model's deficiencies in capturing multivariate interrelationships. Furthermore, it should be stressed that even where bias-correction improves the calibration sample fit, there is no reason to assume that the model bias is constant over time, so any bias-corrected projections from a climate model outside the calibration sample are still suspect (Chen et al., 2015).

Table 3
Regressions of sea ice extent on Cumulative CO_2 Emissions.

	Sea ice extent		
	September	Annual Average	March
Intercept (million km^2)	6.068	11.427	15.284
	(.080)	(.032)	(.040)
Sensitivity (m^2/t CO_2)	−3.112	−2.072	−1.563
	(.253)	(.010)	(.126)
R^2	.79	.92	.80
NIFA CO_2 level	2675	6079	10187
NIFA Year (SSP2-4.5)	2042		
NIFA Year (SSP3-7.0)	2039	2089	

Notes: Estimated coefficients and R^2's are shown from regressions of sea ice extent (SIE) on demeaned Cumulative CO_2 Emissions since 1850. Standard errors are in parentheses. Intercepts are reported in million km^2. Sensitivity or slope coefficients for cumulative CO_2 emissions since 1850 are shown in m^2 per ton of CO_2 (which is equivalent to thousands km^2 per Gt CO_2). Extrapolated dates of a nearly ice-free Arctic (NIFA) and the associated CO_2 levels are shown assuming the SSP2-4.5 and SSP3-7.0 scenario paths. The sample period is 1979–2019. See text for details.

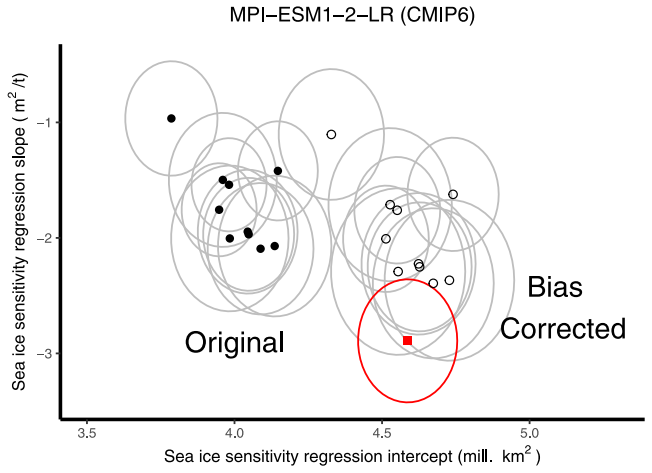

Fig. 6. September sea ice sensitivity of a bias-corrected CMIP6 model.
Notes: The sea ice sensitivity regression intercept and slope for the observed September data (1979–2019) are denoted by a red square. Similar intercepts and slopes estimated from single simulation runs of the MPI- ESM1-2-LR (CMIP6) ensemble are shown as black circles. Intercept and slope estimates from bias-corrected simulation runs are shown as white circles. Each ellipse is a 95% confidence interval for a coefficient pair based on sample variability.

More broadly, these results raise serious questions about the widespread use of bias-corrected model simulations. The popular univariate bias corrections correct one physical variable at one location during a given time period and will thus fail to reproduce the inter-variable, spatial, and temporal dependencies of the observations. Furthermore, by ignoring the climate model's cross-variable correlations and intertemporal connections, a bias correction jettisons the very structural connections that might give a climate model a forecasting edge over statistical methods. In addition, working only with bias-corrected output risks losing sight of the size and nature of the underlying biases. Accordingly, bias correction of climate model output as a post-processing step may be better viewed as an ad hoc quick fix. It may be acceptable for some applied work, but a well-founded solution will require better understanding of the sources of any biases, which may provide a path to improve the climate model projections.

6. Concluding remarks

The substantial differences in Arctic sea ice sensitivity between CMIP5/6 models on the one hand, and the observational record on the other, imply that the climate models do not adequately capture the underlying physical processes and feedback mechanisms in the Arctic. Of course, the connection between anthropogenic greenhouse gas (GHG) emissions and sea ice coverage is very complex. Atmospheric GHG affect air and ocean temperature and circulation patterns, cloud cover and albedo, and precipitation — all with varying seasonality. As a result, there is still much uncertainty as to why the large-scale climate models fail to capture the extent of the overall downward trend in Arctic sea ice. The type of high-level statistical results presented here may be of use in tuning the climate models or identifying problematic aspects of the models.

The fact that climate models underestimate the sensitivity of arctic sea ice to carbon emissions suggests that the Arctic Ocean will lose its sea ice or "turn blue" at the end of the summer season sooner than predicted by climate models. This is precisely the conclusion at which Diebold and Rudebusch (2022) arrived when comparing climate models to climate data using very different tools than those developed and used in this paper. Furthermore, an early arrival of a seasonally ice-free Arctic will likely have important follow-on implications for the pace of climate change around the world.

Acknowledgments

For comments and/or assistance we thank the Editor and three anonymous referees, Max Goebel, Philippe Goulet Coulombe, Aaron Mora Melendez, Jack Mueller, Gladys Teng, Boyuan Zhang, and the Penn Econometrics Research Group. The usual disclaimer applies.

Appendix A. Data

A.1. Observed data

A.1.1. Arctic sea ice area and extent

Monthly average area and extent data are from the National Snow and Ice Data Center (https://nsidc.org/data/G02135/versions/3), measured in millions of square kilometers. The December 1987 and January 1988 observations are missing because of satellite problems. We interpolate those observations with fitted values from a regression on trend and monthly dummies estimated using the full data sample. The reported values for Arctic sea ice area do not include the area near the pole not imaged by the satellite sensor (the "pole hole"), but, to maintain comparability to climate model output, the pole hole has been added. Its area is 1.19 million square kilometers from 1979 through August 20, 1987, 0.31 million square kilometers from 21 August 1987 through December 2007, and 0.029 million square kilometers from January 2008 onward.

A.1.2. CO_2 emissions

Global annual CO_2 emissions data are from the 2020 Global Carbon Budget Project (https://www.icos-cp.eu/science-and-impact/global-carbon-budget/2020.), Fossil emissions excluding carbonation are used, measured in billions of tons of carbon dioxide per year ($GtCO_2$/yr). A cumulative CO_2 emissions series is then created, using base year 1850.

Table 4
September sea ice individual model results (Cumulative CO_2 Emissions since 1850).

Model	Intercept (mill. km^2)			Slope (m^2/t)			Joint test
	$\hat{\alpha}_i$	s.e.	$P(\hat{\alpha}_i = \hat{\alpha}_0)$	$\hat{\beta}_i$	s.e.	$P(\hat{\beta}_i = \hat{\beta}_0)$	
Observed	4.587	0.066	–	−2.891	0.209	–	–
ACCESS1-0	4.849	0.097	0.028	−1.941	0.307	0.013	0.005
ACCESS1-3	4.869	0.095	0.017	−2.633	0.301	0.482	0.045
BNU-ESM	2.329	0.066	0.000	−2.163	0.209	0.016	0.000
CanESM2_R1	2.416	0.085	0.000	−2.422	0.271	0.174	0.000
CanESM2_R2	2.494	0.085	0.000	−2.087	0.269	0.021	0.000
CanESM2_R3	2.559	0.071	0.000	−2.192	0.224	0.025	0.000
CanESM2_R4	2.429	0.079	0.000	−2.763	0.252	0.695	0.000
CanESM2_R5	2.464	0.092	0.000	−2.277	0.291	0.091	0.000
CCSM4_R1	5.335	0.116	0.000	−2.347	0.369	0.203	0.000
CCSM4_R2	5.660	0.083	0.000	−1.423	0.263	0.000	0.000
CCSM4_R3	5.285	0.096	0.000	−1.669	0.305	0.001	0.000
CCSM4_R4	5.286	0.071	0.000	−1.337	0.224	0.000	0.000
CCSM4_R5	5.657	0.080	0.000	−1.848	0.252	0.002	0.000
CCSM4_R6	5.435	0.077	0.000	−2.133	0.244	0.021	0.000
CESM1-BGC	5.323	0.083	0.000	−2.913	0.264	0.950	0.000
CESM1-CAM5	5.498	0.092	0.000	−2.576	0.292	0.382	0.000
CESM1-CAM5-1-FV2	5.913	0.101	0.000	−1.762	0.319	0.004	0.000
CESM1-WACCM_R1	5.435	0.077	0.000	−2.133	0.244	0.021	0.000
CESM1-WACCM_R2	7.648	0.065	0.000	−1.486	0.207	0.000	0.000
CESM1-WACCM_R3	7.614	0.059	0.000	−0.916	0.186	0.000	0.000
CESM1-WACCM_R4	7.538	0.041	0.000	−0.856	0.131	0.000	0.000
CMCC-CESM	7.808	0.043	0.000	−1.184	0.138	0.000	0.000
CMCC-CM	8.772	0.052	0.000	−2.988	0.163	0.717	0.000
CMCC-CMS	7.392	0.039	0.000	−0.998	0.123	0.000	0.000
CNRM-CM5_R1	4.617	0.098	0.798	−2.479	0.310	0.274	0.530
CNRM-CM5_R2	4.057	0.106	0.000	−1.491	0.335	0.001	0.000
CNRM-CM5_R4	4.324	0.105	0.038	−2.328	0.334	0.157	0.044
CNRM-CM5_R6	4.520	0.088	0.543	−2.856	0.279	0.921	0.826
CNRM-CM5_R10	4.178	0.154	0.017	−4.291	0.487	0.010	0.002
CSIRO-Mk3-6-0_R1	9.281	0.027	0.000	−1.069	0.087	0.000	0.000
CSIRO-Mk3-6-0_R2	9.417	0.034	0.000	−0.779	0.107	0.000	0.000
CSIRO-Mk3-6-0_R3	9.293	0.026	0.000	−1.125	0.084	0.000	0.000
CSIRO-Mk3-6-0_R4	9.695	0.033	0.000	−0.876	0.106	0.000	0.000
CSIRO-Mk3-6-0_R5	9.645	0.026	0.000	−1.139	0.083	0.000	0.000
CSIRO-Mk3-6-0_R6	9.728	0.029	0.000	−0.979	0.092	0.000	0.000
CSIRO-Mk3-6-0_R7	9.405	0.036	0.000	−1.426	0.116	0.000	0.000
CSIRO-Mk3-6-0_R8	9.506	0.036	0.000	−1.478	0.113	0.000	0.000
CSIRO-Mk3-6-0_R9	9.375	0.035	0.000	−0.364	0.112	0.000	0.000
CSIRO-Mk3-6-0_R10	9.525	0.045	0.000	−1.017	0.142	0.000	0.000
EC-EARTH_R1	6.505	0.046	0.000	−1.687	0.146	0.000	0.000
EC-EARTH_R2	6.658	0.056	0.000	−1.474	0.177	0.000	0.000
EC-EARTH_R3	6.748	0.070	0.000	−1.900	0.221	0.002	0.000
EC-EARTH_R4	9.695	0.033	0.000	−0.876	0.106	0.000	0.000
EC-EARTH_R5	7.654	0.123	0.000	2.729	0.391	0.000	0.000
EC-EARTH_R6	6.681	0.071	0.000	−1.046	0.224	0.000	0.000
EC-EARTH_R8	6.754	0.089	0.000	−1.278	0.283	0.000	0.000
EC-EARTH_R9	6.686	0.061	0.000	−1.300	0.194	0.000	0.000
EC-EARTH_R10	6.656	0.052	0.000	−1.667	0.165	0.000	0.000
EC-EARTH_R12	6.541	0.069	0.000	−1.833	0.218	0.001	0.000
EC-EARTH_R14	6.903	0.062	0.000	−0.976	0.195	0.000	0.000
FGOALS-g2	6.803	0.061	0.000	−0.574	0.193	0.000	0.000
FIO-ESM_R1	4.969	0.073	0.000	−0.988	0.233	0.000	0.000
FIO-ESM_R2	5.320	0.055	0.000	−1.182	0.174	0.000	0.000
FIO-ESM_R3	5.007	0.076	0.000	−1.222	0.243	0.000	0.000
GFDL-CM3	5.343	0.095	0.000	−3.547	0.303	0.079	0.000
GFDL-ESM2G	6.820	0.077	0.000	−1.791	0.245	0.001	0.000
GFDL-ESM2M	5.168	0.088	0.000	−0.475	0.279	0.000	0.000
GISS-E2-H	1.399	0.095	0.000	−2.093	0.301	0.032	0.000
GISS-E2-H-CC	1.588	0.104	0.000	−1.286	0.331	0.000	0.000
GISS-E2-R_R1	2.429	0.091	0.000	−2.037	0.288	0.019	0.000
GISS-E2-R_R2	2.445	0.084	0.000	−2.478	0.268	0.228	0.000
HadGEM2-ES_R1	3.590	0.081	0.000	−3.054	0.257	0.624	0.000
HadGEM2-ES_R2	3.946	0.080	0.000	−2.079	0.255	0.016	0.000
HadGEM2-ES_R3	3.409	0.093	0.000	−2.271	0.294	0.090	0.000
HadGEM2-ES_R4	3.617	0.081	0.000	−3.359	0.258	0.164	0.000
IPSL-CM5A-LR_R1	5.902	0.074	0.000	−2.205	0.235	0.032	0.000
IPSL-CM5A-LR_R2	5.238	0.083	0.000	−1.503	0.264	0.000	0.000
IPSL-CM5A-LR_R3	6.062	0.066	0.000	−2.083	0.209	0.008	0.000
IPSL-CM5A-LR_R4	5.867	0.069	0.000	−1.818	0.218	0.001	0.000
IPSL-CM5A-MR	4.226	0.083	0.001	−2.269	0.262	0.067	0.001

(*continued on next page*)

Table 4 (*continued*).

Model	Intercept (mill. km^2)			Slope (m^2/t)			Joint test
	$\hat{\alpha}_i$	s.e.	$P(\hat{\alpha}_i = \hat{\alpha}_0)$	$\hat{\beta}_i$	s.e.	$P(\hat{\beta}_i = \hat{\beta}_0)$	
IPSL-CM5B-LR	8.032	0.064	0.000	−1.117	0.204	0.000	0.000
MIROC5_R1	5.820	0.086	0.000	−2.525	0.271	0.289	0.000
MIROC5_R2	5.880	0.054	0.000	−2.086	0.170	0.004	0.000
MIROC5_R3	5.888	0.065	0.000	−1.864	0.206	0.001	0.000
MIROC-ESM	4.719	0.060	0.141	−1.815	0.189	0.000	0.000
MIROC-ESM-CHEM	5.157	0.096	0.000	−2.751	0.304	0.704	0.000
MPI-ESM-LR_R1	4.840	0.071	0.011	−1.955	0.224	0.003	0.001
MPI-ESM-LR_R2	4.915	0.094	0.006	−1.477	0.299	0.000	0.000
MPI-ESM-LR_R3	4.835	0.054	0.005	−1.293	0.171	0.000	0.000
MPI-ESM-MR	4.890	0.068	0.002	−1.755	0.216	0.000	0.000
MRI-CGCM3	5.076	0.149	0.004	−1.330	0.474	0.003	0.000
MRI-ESM1	5.015	0.162	0.017	−2.437	0.513	0.415	0.041
NorESM1-M	6.670	0.053	0.000	−1.498	0.167	0.000	0.000
NorESM1-ME	7.306	0.064	0.000	−0.991	0.202	0.000	0.000

Notes: The sea ice sensitivity regression intercept and slope estimated from the observed September data (1979–2019) are shown on the first line of the table. Sea ice sensitivity regression intercepts and slopes estimated from CMIP5 models are shown in the $\hat{\alpha}_i$ and $\hat{\beta}_i$ columns respectively along with standard errors for each estimate. The columns $P(\hat{\alpha}_i = \hat{\alpha}_0)$ and $P(\hat{\beta}_i = \hat{\beta}_0)$ show the p-values for the tests $H_0 : a = 0$ and $H_0 : b = 0$ respectively. The a and b coefficients are estimated from the regression $SIA_t = \alpha_i + \beta_i CO2_t + aO_t + bO_t CO2_t + \varepsilon_t$ performed on model and observed pooled data, where O_t is a dummy variable for observed data. The last column shows the p-value of the joint test $H_0 : (a, b) = (0, 0)$.

A.2. Climate model data

A.2.1. CMIP5 climate model data

The sea ice area data for individual models of phase five of the Coupled Model Intercomparison Project (CMIP5) are based on publicly available output from the replication file for Notz and Stroeve (2016). The historical scenario data range from 1860 to 2005, and the model data for RCP8.5 range from 2006 to 2100.

A.2.2. CMIP6 climate model data

The sea ice area data for 29 single run models of phase six of the Coupled Model Intercomparison Project (CMIP6) are taken from the replication file for Bonan et al. (2021) (https://zenodo.org/record/5177172). The historical scenario data range from 1860 to 2005, and the model data for SSP5-8.5 range from 2006 to 2100.

Data for multi-run CMIP6 models were directly queried from the World Climate Research Program (WCRP) data repository (https://esgf-node.llnl.gov/search/cmip6/). Data at monthly frequency of sea ice concentration for the historical, SSP1-2.6, SSP2-4.5, SSP3-7.0 and SSP5-8.5 experiments were queried for the CanESM5, MPI-ESM1-2-LR, CNRM-CM6-1, EC-Earth3, IPSL-CM6A-LR and MIROC6 models.

To obtain time series from the queried data, the following steps are necessary: (i) convert raw gridded data in `netcdf4` format to `netcdf-classic`; (ii) use Climate Data Operators (CDO) (https://code.mpimet.mpg.de/projects/cdo) to convert gridded data from the `netcdf-classic` files into monthly Northern Hemispheric SIA and SIE values; (iii) convert the transformed files into monthly time series. This was done in R with the resulting series stored into `csv` files for further use.

The resulting series contain Northern Hemisphere annual SIA and SIE from 1850–2100 for each model ensemble. In such series the historical range is from January 1850 to December 2014, and the SSP simulations (SSP1-2.6, SSP2-4.5, SSP3-7.0 and SSP5-8.5) start in January 2015.

Appendix B. Sensitivity in observed sea ice extent

Here observed-data Arctic sea ice sensitivity is examined using an alternative measure of Arctic sea ice, sea ice extent (SIE), as ICE_t. Monthly average SIE data from the National Snow and Ice Data Center (NSIDC) are used, January 1979–December 2019. These data use the NASA team algorithm to convert microwave brightness readings into ice coverage estimates for each grid cell, after which SIE is then calculated as the total area of all cells with at least 15% coverage.

The SIE results are shown in Fig. 7 and Table 3. They parallel the SIA results shown in the main text in Fig. 1 and Table 1, although, because SIE is invariably a bit higher than SIA by virtue of its construction, the September sea ice NIFA and IFA dates are pushed about 7 or 8 years later.

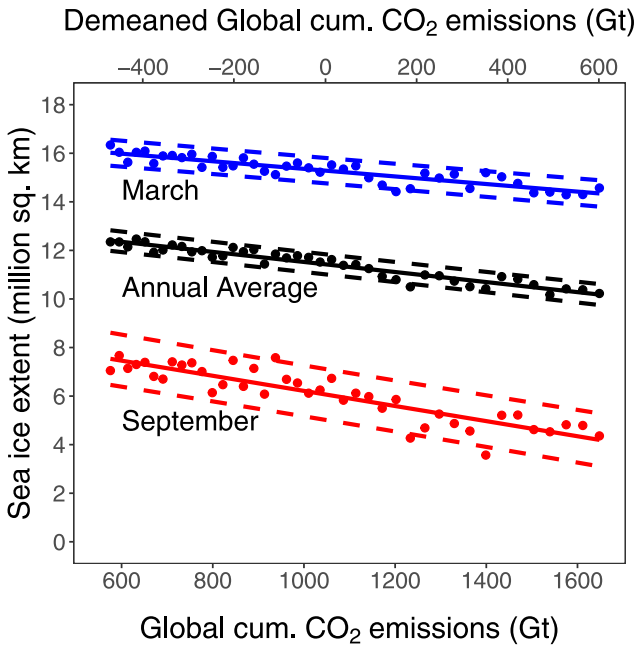

Fig. 7. Arctic sea ice extent and CO_2.
Notes: Arctic sea ice extent (in million km^2) is shown against global cumulative CO2 emissions in Gt. March, annual average, and September observations are shown in blue, black, and red, respectively. Dashed lines are 95% prediction intervals accounting for parameter estimation uncertainty. Carbon scales are shown in both demeaned (top scale) and non-demeaned (bottom scale) form. The sample period is 1979–2019. See text for details. (For interpretation of the references to color in this figure legend, the reader is referred to the web version of this article.)

Appendix C. Detailed CMIP5 regression results

See Table 4.

Appendix D. Supplementary material

Supplementary material related to this article can be found online at https://doi.org/10.1016/j.eneco.2023.107012.

References

Bonan, D.B., Schneider, T., Eisenman, I., Wills, R.C.J., 2021. Constraining the date of a seasonally ice-free arctic using a simple model. Geophys. Res. Lett. 48 (18), e2021GL094309.

Chen, J., Brissette, F.P., Lucas-Picher, P., 2015. Assessing the limits of bias-correcting climate model outputs for climate change impact studies. J. Geophys. Res.: Atmos. 120 (3), 1123–1136.

Diebold, F.X., Goebel, M., Goulet Coulombe, P., Rudebusch, G.D., Zhang, B., 2021. Optimal combination of arctic sea ice extent measures: A dynamic factor modeling approach. Int. J. Forecast. 37, 1509–1519.

Diebold, F.X., Rudebusch, G.D., 2022. Probability assessments of an ice-free arctic: Comparing statistical and climate model projections. J. Econometrics 231, 520–534.

Diebold, F.X., Rudebusch, G.D., Goebel, M., Goulet Coulombe, P., Zhang, B., 2023. When will arctic sea ice disappear? Projections of area, extent, thickness, and volume. J. Econometrics 236, 105479.

Ehret, U., Zehe, E., Wulfmeyer, V., Warrach-Sagi, K., Liebert, J., 2012. Should we apply bias correction to global and regional climate model data? HESS Opinions, Hydrol. Earth Syst. Sci. 16 (9), 3391–3404.

François, B., Vrac, M., Cannon, A.J., Robin, Y., Allard, D., 2020. Multivariate bias corrections of climate simulations: Which benefits for which losses? Earth Syst. Dyn. 11 (2), 537–562.

Guarino, M.V., Sime, L.C., Schroeder, D., Malmierca-Vallet, I., Rosenblum, E., Ringer, M., Ridley, J., Feltham, D., Bitz, C., Steig, E.J., Wolff, E., Stroeve, J., Sellar, A., 2020. Sea-ice free arctic during the last interglacial supports fast future loss. Nature Clim. Change 10, 928–932.

IPPC, 2023. In: Masson-Delmotte, V., Zhai, P., Pirani, A., Connors, S.I., Péan, C., Berger, S., Caud, N., Chen, Y., Goldfarb, L., Gomis, M., Huang, I.M., Leitzell, K., Lonnoy, E., Matthews, J.B.R., Maycock, T.K., Waterfield, T., Yelekçi, O., Yu, R., Zhou, B. (Eds.), Climate Change 2021: The Physical Science Basis. Contribution of Working Group I to the Sixth Assessment Report of the Intergovernmental Panel on Climate Change. Cambridge University Press.

Ivanov, M.A., Luterbacher, J., Kotlarski, S., 2018. Climate model biases and modification of the climate change signal by intensity-dependent bias correction. J. Clim. 31 (16), 6591–6610.

Jahn, A., Kay, J.E., Holland, M.M., Hall, D.M., 2016. How predictable is the timing of a summer ice-free arctic? Geophys. Res. Lett. 43 (17), 9113–9120.

Johannessen, O.M., 2008. Decreasing arctic sea ice mirrors increasing CO2 on decadal time scale. Atmospheric Ocean. Sci. Lett. 1 (1), 51–56.

Kiefer, N.M., Salmon, M., 1983. Testing normality in econometric models. Econom. Lett. 11 (1–2), 123–127.

Kusumastuti, C., Jiang, Z., Mehrotra, R., Sharma, A., 2022. Correcting systematic bias in climate model simulations in the time-frequency domain. Geophys. Res. Lett. 49 (19), e2022GL100550.

Matthews, H.D., Gillett, N.P., Stott, P.A., Zickfield, K., 2009. The proportionality of global warming to cumulative carbon emissions. Nature 459 (7248), 829–832.

Melia, N., Haines, K., Hawkins, E., 2015. Improved arctic sea ice thickness projections using bias-corrected CMIP5 simulations. Cryosphere 9 (6), 2237–2251.

Notz, D., SIMIP Community, 2020. Arctic sea ice in CMIP6. Geophys. Res. Lett. 47 (10), e2019GL086749.

Notz, D., Stroeve, J., 2016. Observed arctic sea-ice loss directly follows anthropogenic CO2 emission. Science 354 (6313), 747–750.

Notz, D., Stroeve, J., 2018. The trajectory towards a seasonally ice-free arctic ocean. Curr. Climate Change Rep. 4 (4), 407–416.

Olonscheck, D., Notz, D., 2017. Consistently estimating internal climate variability from climate model simulations. J. Clim. 30 (23), 9555–9573.

Otto, F.E., Massey, N., van Oldenborgh, G.J., Jones, R.G., Allen, M.R., 2012. Reconciling two approaches to attribution of the 2010 Russian heat wave. Geophys. Res. Lett. 39 (4), L04702.

Quandt, R.E., 1960. Tests of the hypothesis that a linear regression system obeys two separate regimes. J. Am. Stat. Assoc. 55, 324–330.

Rosenblum, E., Eisenman, I., 2017. Sea ice trends in climate models only accurate in runs with 49 biased global warming. J. Clim. 30 (16), 6265–6278.

Stock, J.H., Sims, C.A., Watson, M.W., 1990. Inference in linear time series models with some unit roots. Econometrica 58 (1), 113–144.

Stroeve, J., Holland, M.M., Meier, W., Scambos, T., Serreze, M., 2007. Arctic sea ice decline: Faster than forecast. Geophys. Res. Lett. 34 (9), L09501.

Stroeve, J., Notz, D., 2018. Changing state of arctic sea ice across all seasons. Environ. Res. Lett. 13 (10), 103001.

Stroeve, J.C., Serreze, M.C., Holland, M.M., Kay, J.E., Malanik, J., Barrett, A.P., 2012. The arctic's rapidly shrinking sea ice cover: A research synthesis. Clim. Change 110 (3), 1005–1027.

Turner, J., Bracegirdle, T.J., Phillips, T., Marshall, G.J., Hosking, J.S., 2013. An initial assessment of antarctic sea ice extent in the CMIP5 models. J. Clim. 26 (5), 1473–1484.

Winton, M., 2011. Do climate models underestimate the sensitivity of northern hemisphere sea ice cover? J. Clim. 24 (15), 3924–3934.